ELSEVIER

www.elsevier.com/locate/carres

Carbohydrate Research 335 (2001) 261–273

CARBOHYDRATE RESEARCH

Modeling of deoxy- and dideoxyaldohexopyranosyl ring puckering with MM3(92)

William M. Rockey,[a] Michael K. Dowd,[b] Peter J. Reilly,[a,*] Alfred D. French[b]

[a]*Department of Chemical Engineering, Iowa State University, Ames, IA 50011, USA*
[b]*Southern Regional Research Center, U.S. Department of Agriculture, New Orleans, LA 70179, USA*

Received 18 June 2001; accepted 22 August 2001

Abstract

Extensive variations of the ring structures of three deoxyaldohexopyranoses, L-fucose, D-quinovose, and L-rhamnose, and four dideoxyaldohexopyranoses, D-digitoxose, abequose, paratose, and tyvelose, were studied by energy minimization with the molecular mechanics algorithm MM3(92). Chair conformers, $^4C_1$ in D-quinovose and the equivalent $^1C_4$ in L-fucose and L-rhamnose, overwhelmingly dominate in the three deoxyhexoses; in the D-dideoxyhexoses, $^4C_1$ is again dominant, but with increased amounts of $^1C_4$ forms in the α anomers of the three 3,6-dideoxyhexoses, abequose, paratose, and tyvelose and in both α and β anomers of the 2,6-dideoxyhexose D-digitoxose. In general, modeled proton–proton coupling constants agreed well with experimental values. Computed anomeric ratios strongly favor the β configuration except for D-digitoxose, which is almost equally divided between α and β configurations, and L-rhamnose, where the β configuration is somewhat favored. MM3(92) appears to overstate the prevalence of the equatorial β anomer in all three deoxyhexoses, as earlier found with fully oxygenated aldohexopyranoses. © 2001 Published by Elsevier Science Ltd.

Keywords: Abequose; Digitoxose; Fucose; MM3; Molecular mechanics; Paratose; Quinovose; Rhamnose; Ring puckering; Tyvelose

1. Introduction

Hexoses, particularly aldohexoses, are found primarily as pyranoses in solution and in most oligo- and polysaccharides. Furthermore, these pyranosyl rings usually exist in the chair form, although other forms do appear.

The structures of many hexosyl rings have been studied. This can be accomplished in two ways, by experimentation, chiefly by NMR[1–3] or diffraction,[4] and by computation.[5–8] Obviously experimentation gives a conclusive result, but one that is either a conformational average, if by NMR, or a single snapshot of the possible accessible space, if by diffraction. Computation, in contrast, allows a more thorough investigation of the whole conformational surface and gives a good insight into the various conformers that may be present in small amounts. However, it is subject to many simplifications and approximations. A combination of these methods often proves very helpful in understanding hexosyl conformations.

Most of the work on hexosyl ring structures has been conducted on those having the formula $C_6H_{12}O_6$, with other hexoses including several lacking one or more hydroxyl groups

* Corresponding author. Tel.: +1-515-2945968; fax: +1-515-2942689.
E-mail address: reilly@iastate.edu (P.J. Reilly).

0008-6215/01/$ - see front matter © 2001 Published by Elsevier Science Ltd.
PII: S0008-6215(01)00240-3

being comparatively neglected. Nine naturally occurring deoxy- and dideoxyaldohexoses without 6-OH groups, fucose (6-deoxygalactose), quinovose (6-deoxyglucose), rhamnose (6-deoxymannose), digitoxose (2,6-dideoxy-*ribo*-hexose or 2,6-dideoxyallose), abequose (3,6-dideoxy-D-*xylo*-hexose or 3,6-dideoxy-D-galactose), colitose (3,6-dideoxy-L-*xylo*-hexose or 3,6-dideoxy-L-galactose), paratose (3,6-dideoxy-D-*ribo*-hexose or 3,6-dideoxy-D-glucose), tyvelose (3,6-dideoxy-D-*arabino*-hexose or 3,6-dideoxy-D-mannose), and ascarylose (3,6-dideoxy-L-*arabino*-hexose or 3,6-dideoxy-L-mannose) (Fig. 1), have been subjected to at least a modicum of research. The first four encompass both D- and L-forms, while abequose and colitose are mirror images of each other, as are tyvelose and ascarylose. Paratose has no naturally occurring corresponding L-form.

A number of deoxy- and dideoxyhexoses have attracted interest in recent years because of their biochemical roles in disease and due to their presence in cardiac glycosides or in antigenic lipopolysaccharides and glycoproteins. For example, L-fucose has been investigated as a potential agent to prevent tumor cell growth[9] and as an anti-inflammatory drug to alleviate rheumatoid arthritis.[10] Quinovose is found in leaves of *Calonyction aculeatum* as part of the plant hormone calonyctin A,[11] and L-quinovose is part of phenazine alkaloids from marine actinomycetes.[12] L-Rhamnose is the sugar component of the cardiac glycoside ouabain, which has inotropic effects.[13] Of the five 3,6-dideoxyhexoses that occur naturally, abequose, colitose, paratose, and tyvelose are in the O-antigen lipopolysaccharides of *Salmonella enterica*, and these four plus ascarylose are present in *Yersinia pseudotuberculosis*.[14] A thorough review of deoxyhexosyl biosynthesis appeared some years ago.[15] More recently, the identification and sequencing of the *Salmonella typhi* and *Y. pseudotuberculosis* genes that code for CDP-D-tyvelose 2-

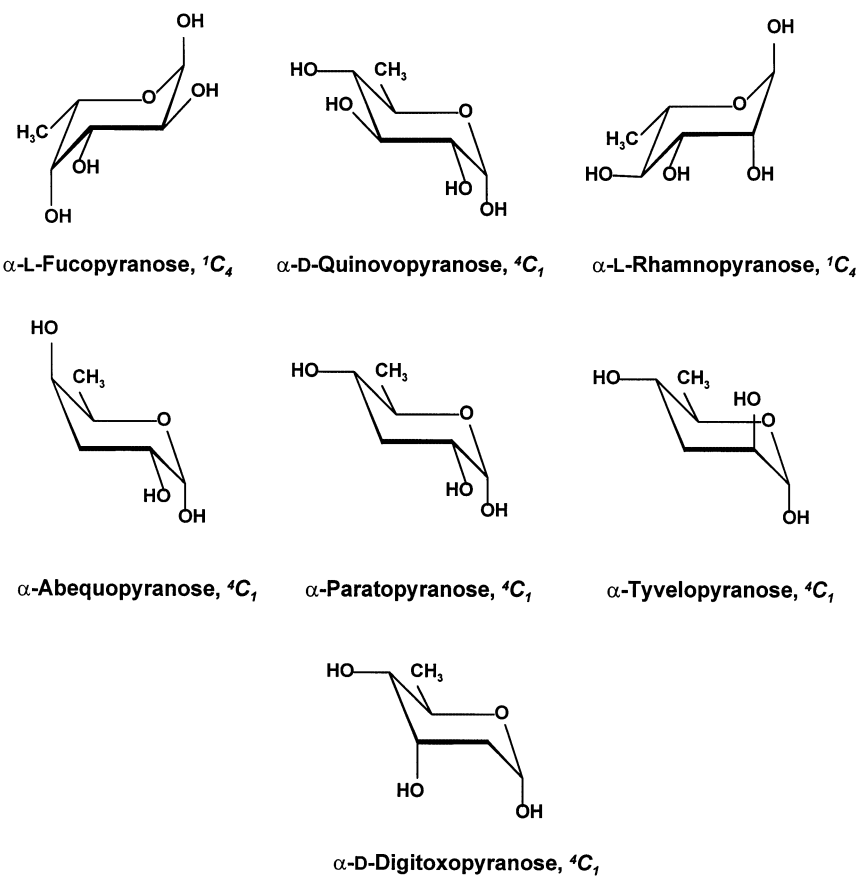

Fig. 1. Most prevalent pyranosyl conformers of seven deoxy- and dideoxyaldohexoses.

epimerase has inspired mechanistic studies of the in vivo synthesis of tyvelose.[16]

The configuration of monosaccharide units in a cardiac glycoside significantly affects the reaction kinetics of that glycoside with Na^+,K^+-ATPase, the enzyme that triggers the familiar cardiac effects of those drugs. Fullerton et al.[17] reported that glycosides having sugars with an equatorial 4-OH group, such as α-L-rhamnose in ouabain and β-D-digitoxose bound to digitoxigenin, display a much higher bioreactivity than those with axial 4-OH groups. They further reported an increase in activity caused by an equatorial 2-OH and a decrease in activity due to the presence of a hydroxyl group on C-6.

These results suggest that ring structures of deoxy- and dideoxyhexoses could also affect bioreactivity, and that a greater knowledge of the fractions of different conformational and anomeric forms of these sugars would be helpful for future pharmacological and biochemical studies.

A number of studies have been conducted on the ring structures of these nine deoxy- and dideoxyaldohexoses. The crystal structures of the pyranosyl forms of fucose,[18–23] rhamnose,[24–35] digitoxose,[36–38] and tyvelose[39] have been determined. In addition, the NMR spectra of both anomers of the pyranosyl forms of L-fucose,[40,41] D-quinovose,[40,41] L-rhamnose,[30,40–42] D-digitoxose,[43–46] and tyvelose,[47] as well as the pyranosyl forms of α-tyvelose[39] and β-paratose,[48] are available. In what is apparently the only computational study of the ring structures of any of these nine carbohydrates, Csonka et al.[49] used ab initio methods to elucidate the conformational space of the $^1C_4$ conformer of α-L-fucose, starting with 17 minima determined by molecular mechanics.

The molecular mechanics program MM3,[50–52] employed in this study, has previously been used to determine the relative amounts of the ring conformers of the pyranosyl forms of the eight aldohexoses[53] and the nine inositols,[54] both furanosyl and pyranosyl forms of the ketohexoses psicose[55] and fructose[56] and the aldopentoses ribose and 2-deoxyribose,[57] the pyranosyl forms of the aldopentoses arabinose, lyxose, and xylose,[58] and the furanosyl form of arabinose.[59]

We report in this article a computational investigation using MM3(92) of the conformations of the pyranosyl rings of three deoxyaldohexoses, L-fucose, D-quinovose, and L-rhamnose, and of four D-dideoxyaldohexoses, D-digitoxose, abequose, paratose, and tyvelose. Both α and β anomers of the seven sugars have been studied. Such a study encompasses D-fucose, L-quinovose, D-rhamnose, L-digitoxose, colitose, and ascarylose through mirror symmetry. Computed steric energies, fractions of ring conformers and anomers, and hydrogen–hydrogen coupling constants of the various hexoses are reported.

2. Computational methods

The computational protocol was largely unchanged from previous studies.[53–55] All simulations were executed on an SGI Orgin 2000 multiprocessor system using MM3(92). Some elevation of the dielectric constant is necessary to reduce the strength of hydrogen bonds to better mimic condensed-phase systems. Therefore a value of 3.0 was specified for all simulations, as it allowed a good fit of crystallographic and NMR data in previous simulations.[60] For each molecule, planar ring structures were generated with all possible staggered exocyclic orientations of the hydroxyl groups. These starting structures numbered 81 (3^4) for the deoxyhexoses and 27 (3^3) for the dideoxyhexoses. The flat rings were oriented in the xy-plane and were subsequently puckered by translating the C-2, C-4, and O-5 ring atoms and all of their non-ring substituents in the z-direction in 0.1-Å increments from -0.8 to $+0.8$ Å. The resulting 4913 (17^3) $\times$ 27 or 81 structures were then submitted to MM3 for structural optimization. The block-diagonal Newton–Raphson energy minimization routine was used with the default convergence criteria to reduce the computational load.

The classification system of Cremer and Pople[61,62] was used to describe the ring shapes of the optimized structures. In this system, hexosyl rings are described by the parameters q, ϕ, and θ, representing puckering amplitude, phase angle, and inversion angle, respectively.

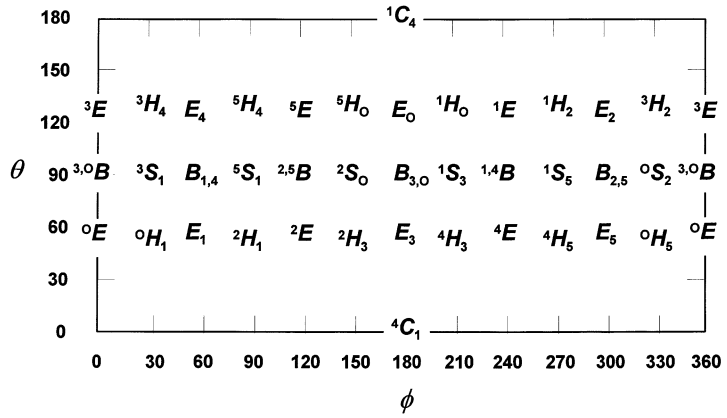

Fig. 2. Locations of characteristic pyranosyl conformers on the surface of the Pickett–Strauss puckering map.

Values of ϕ and θ, together with the MM3 energy, were used to create the plate carée projections of Pickett and Strauss[63,64] for each sugar (Fig. 2). This was achieved by a binning process that sorts the structures within incremental regions of ϕ and θ and identifies the lowest energy structures within each incremental bin. Because the lowest energy forms are all found within a narrow region of q, these maps provide a convenient representation of energy versus conformation.

To locate local minima, the lowest energy conformations from each low-energy area of the Pickett–Strauss surface were reoptimized with all possible staggered orientations of the exo-cyclic substituents. The block-diagonal minimization routine was used, followed by the MM3 full-matrix optimization routine as minima were approached. Since MM3(92) permits ring chirality change during this optimization (this problem has been corrected in later versions), the final optimized structures were checked and if necessary inverted to maintain the chirality of the original anomer. If any of the reoptimized local structures were found in different regions of the Cremer–Pople space, the original regions were considered to have no minima. Hydrogen–hydrogen NMR coupling constants were calculated for each local minimum using the Karplus equations of Haasnoot et al.[65]

3. Results

The Cremer–Pople energy surface plots of the pyranosyl forms of the seven deoxy- and dideoxyaldohexoses calculated by MM3 all have the same overall topology (Fig. 3). Two high-energy ridges with approximate θ values of 60 and 120° extend parallel to each other horizontally along the length of the plots. A low-energy valley spanning approximate θ values of 80–100° divides the ridges, with a number of local-minima skew and skew–boat conformations located in it. The outside slopes of the two ridges incline downward toward their respective borders, where the global minimum and other low-energy chair conformations are found. The differences in the energy surfaces of the various monosaccharides lie in local energy minima and maxima and in the corresponding variations in supra-ground state conformations.

Both anomeric forms of all seven deoxy- and dideoxyhexoses favor chair forms (Table 1). With the five D-sugars (abequose, digitoxose, paratose, quinovose, and tyvelose), this is always the $^4C_1$ conformation, with the second most common form being $^1C_4$. With β-abequose, β-paratose, α- and β-quinovose, and β-tyvelose, the $^4C_1$ form is essentially the only one present. For α-abequose, α- and β-D-digitoxose, α-paratose, and α-tyvelose, there are increasing amounts of the $^1C_4$ conformation, ranging up to 25% of α-paratose. Other conformations do not exceed 0.02% in any case except for 1.4% of $^OS_2$ in α-tyvelose.

L-Fucose and L-rhamnose are overwhelmingly found as $^1C_4$ conformers, equivalent to the $^4C_1$ form in D-sugars (Table 1). The latter is the second most common form in α-L-fucose and α-L-rhamnose, with $^3S_1$ and $^5S_1/^{2,5}B$ being the second forms in β-L-fucose and β-L-

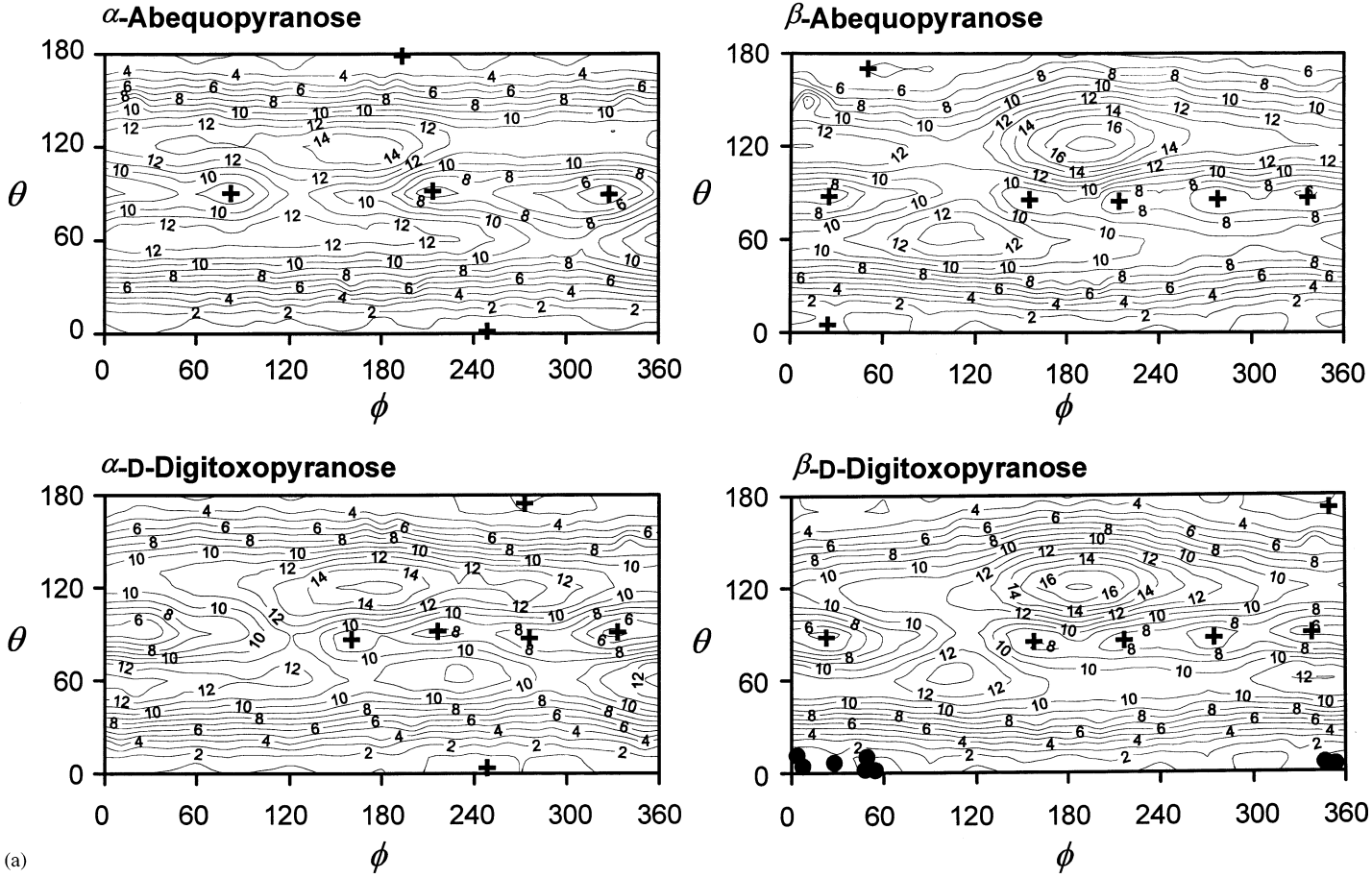

(a)

Fig. 3. MM3-computed ϕ-θ puckering maps for pyranosyl conformers of deoxy- and dideoxyaldohexoses compared to crystal structures. Fucose: α-D-fucopyranose calcium bromide trihydrate,[18] α-L-fucopyranose,[19] α-DL-fucopyranose,[20] methyl α-L-fucopyranoside,[21] methyl 2-*O*-α-L-fucopyranosyl-β-D-galactopyranoside,[22] methyl β-L-fucopyranosyl-(1→4)-α-D-glucopyranoside hemihydrate;[23] rhamnose: α-L-rhamnopyranose monohydrate,[24,25] ouabain, 1β,5,11α,19-tetrahydroxy-3β-*O*-α-L-rhamnopyranosyl-5β,14β-card-20(22)-enolide octahydrate,[26] 14-hydroxy-5β,14β-bufa-4,20,22-triene-amide-3β-*O*-α-L-rhamnoside diethyl ether solvate,[27] benzyl 2,3,6-trideoxy-α-L-*glycero*-hex-2-enopyranosyl-4-ulose-(1→2)-3-*O*-benzoyl-4-*O*-benzyl-α-L-rhamnopyranoside,[28] 3β-*O*-α-L-rhamnopyranosyl-14-hydroxy-14β-bufa-4,20,22-trienolide methanol solvate,[29] 1,2,3-tri-*O*-acetyl-β-L-rhamnopyranoside,[30] 26-*O*-α-L-rhamnopyranosyl-(22*R*,25*S*,26*R*)-22,26-epoxy-6-oxo-5α-cholestan-3β-26-diol-3-*O*-α-L-rhamnopyranosyl-(1→2)-β-D-glucopyranoside monohydrate,[31] methyl α-L-rhamnopyranoside,[32] methyl 2,3,4-tri-*O*-acetyl-α-L-rhamnopyranoside,[33] cyclo[(1→4)-α-L-rhamnopyranosyl-(1→4)-α-D-mannopyranosyl]-tetraoside hydrate octasaccharide,[34] cyclotetrakis[(1→4)-α-D-rhamnopyranosyl-(1→4)-α-L-rhamnopyranosyl] acetone solvate tridecahydrate;[35] digitoxose: β-D-digitoxopyranose,[36] digoxigenin mono-β-D-digitoxopyranoside monohydrate,[37] digitoxigenin bisdis-β-D-digitoxopyranoside ethyl acetate solvate;[38] tyvelose: methyl α-D-tyvelopyranoside.[39] Crystal structures (●), local minima (+).

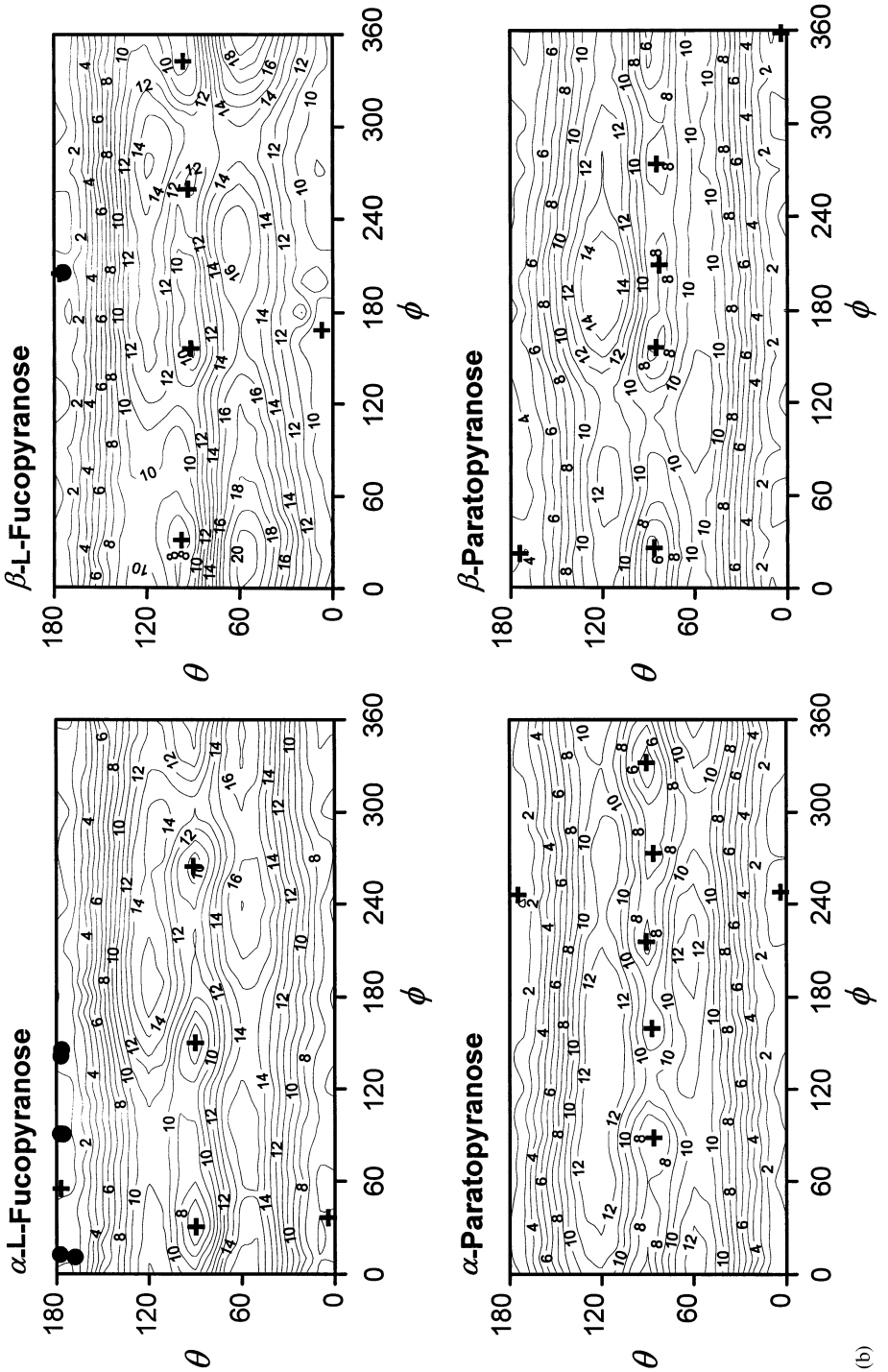

(b)

Fig. 3. (*Continued*)

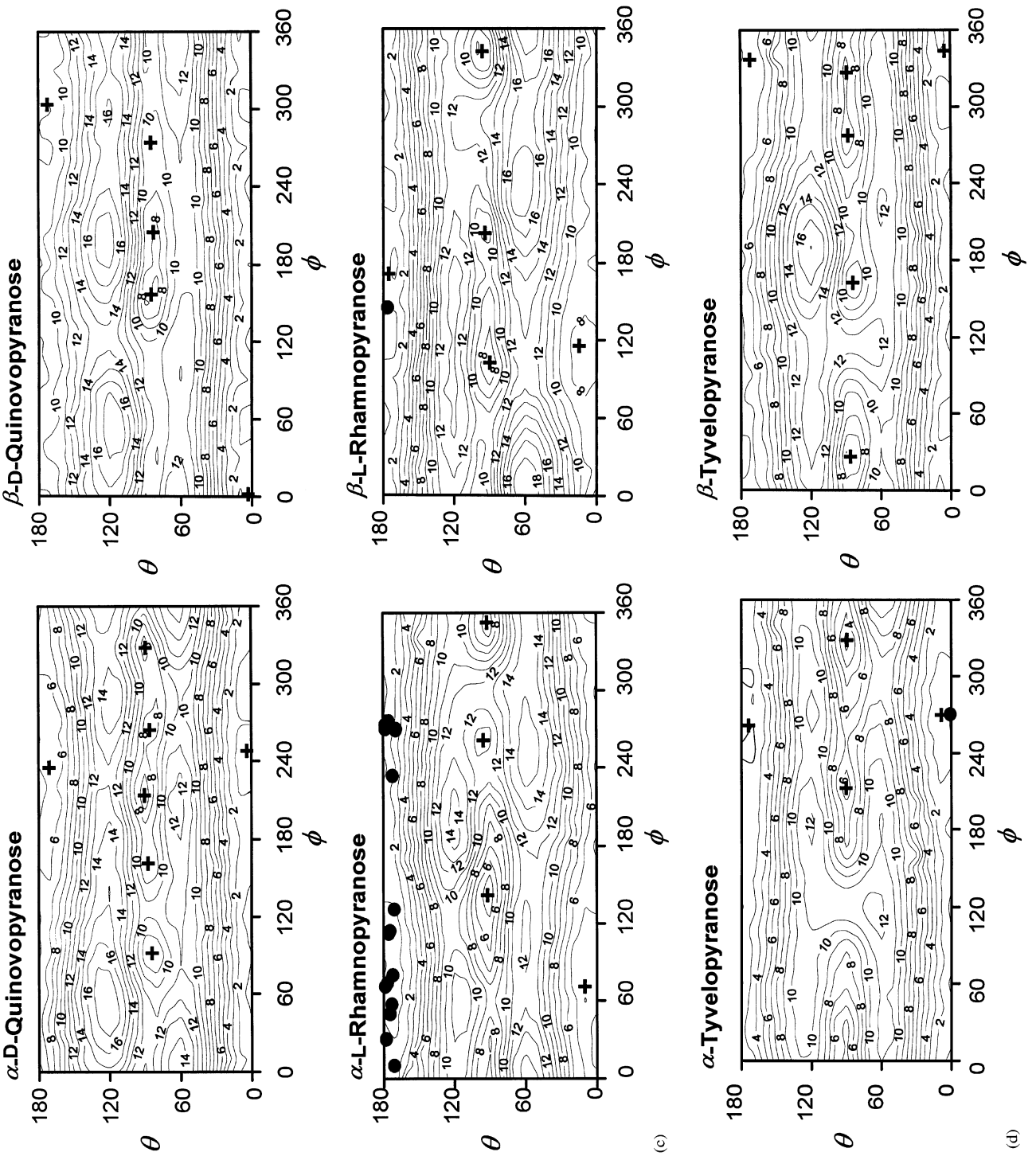

Fig. 3. (*Continued*)

Table 1
Cremer–Pople puckering values and energies of the local minima for deoxy- and dideoxyhexopyranoses calculated by MM3(92) with $\varepsilon = 3.0$

Pyranose	Steric energy (kcal/mol)	Relative energy (kcal/mol)	q (Å)	ϕ (°)	θ (°)	Approx. character form	x_i
α-Abequose	12.15	0.00	0.549	248.7	1.4	$^4C_1$	0.975
	14.37	2.23	0.555	193.6	178.5	$^1C_4$	0.022
	15.71	3.56	0.744	327.9	89.3	$^OS_2$	0.002
	18.20	6.05	0.752	213.5	91.5	$^1S_3$	0.000
β-Abequose	11.36	0.00	0.581	24.7	4.9	$^4C_1$	0.999
	15.90	4.54	0.515	49.9	170.3	$^1C_4$	0.000
	16.75	5.39	0.753	336.5	87.1	$^OS_2$	0.000
	17.03	5.66	0.691	277.7	86.0	$^1S_5/B_{2,5}$	0.000
	17.34	5.97	0.778	24.9	87.8	$^3S_1$	0.000
Average α:	12.21	0.84					0.194
Average β:	11.37	0.00					0.806
α-D-Digitoxose	12.10	0.00	0.557	248.3	3.6	$^4C_1$	0.974
	14.26	2.16	0.553	272.5	174.5	$^1C_4$	0.025
	16.30	4.20	0.771	333.0	91.0	$^OS_2$	0.001
	19.03	6.92	0.768	275.5	87.1	$^1S_5$	0.000
β-D-Digitoxose	12.15	0.00	0.587	348.9	4.7	$^4C_1$	0.969
	14.19	2.04	0.515	349.8	171.5	$^1C_4$	0.031
	16.32	4.17	0.769	22.8	87.8	$^3S_1$	0.001
	17.28	5.13	0.772	338.4	90.0	$^OS_2/^{3,O}B$	0.000
	18.01	5.86	0.745	274.6	87.0	$^1S_5$	0.000
Average α:	12.16	0.00					0.523
Average β:	12.22	0.06					0.477
α-L-Fucose	11.23	0.00	0.553	55.2	177.1	$^1C_4$	1.000
	16.30	5.07	0.540	36.8	4.5	$^4C_1$	0.000
	16.70	5.47	0.763	30.9	89.7	$^3S_1$	0.000
	18.09	6.86	0.741	150.3	90.0	^2S_O	0.000
β-L-Fucose	10.37	0.00	0.585	204.7	176.5	$^1C_4$	1.000
	17.06	6.69	0.694	31.1	97.7	$^3S_1$	0.000
	18.31	7.94	0.712	342.6	96.3	$^OS_2/^{3,O}B$	0.000
Average α:	11.23	0.86					0.188
Average β:	10.37	0.00					0.812
α-Paratose	11.91	0.00	0.566	247.8	3.7	$^4C_1$	0.750
	12.56	0.65	0.541	246.0	174.5	$^1C_4$	0.249
	15.52	3.61	0.751	332.3	90.7	$^OS_2$	0.002
	18.03	6.12	0.743	273.3	86.3	$^1S_5$	0.000
β-Paratose	10.96	0.00	0.595	358.3	3.6	$^4C_1$	0.994
	13.95	2.99	0.495	21.9	174.2	$^1C_4$	0.006
	16.08	5.12	0.760	25.9	86.5	$^3S_1$	0.000
	17.01	6.05	0.714	155.8	85.1	^2S_O	0.000
Average α:	12.08	1.09					0.135
Average β:	10.98	0.00					0.865
α-D-Quinovose	10.47	0.00	0.566	248.0	3.8	$^4C_1$	1.000
	15.15	4.68	0.528	234.9	171.1	$^1C_4$	0.000
	16.51	6.04	0.775	213.6	90.5	$^1S_3$	0.000
	17.57	7.10	0.748	264.3	85.8	$^1S_5$	0.000
β-D-Quinovose	9.39	0.00	0.596	2.0	3.4	$^4C_1$	1.000
	15.43	6.04	0.717	156.7	85.0	^2S_O	0.000
	16.67	7.28	0.710	204.8	82.9	$^1S_3$	0.000
Average α:	10.47	1.08					0.138
Average β:	9.39	0.00					0.862
α-L-Rhamnose	11.18	0.00	0.556	78.7	172.7	$^1C_4$	0.997
	14.93	3.75	0.539	70.8	10.2	$^4C_1$	0.002
	15.10	3.92	0.759	142.4	92.0	$^{2,5}B/^2S_O$	0.000
	17.22	6.04	0.722	352.6	92.0	$^{3,O}B$	0.000

Table 1 (*Continued*)

Pyranose	Steric energy (kcal/mol)	Relative energy (kcal/mol)	q (Å)	ϕ (°)	θ (°)	Approx. character form	x_i
β-L-Rhamnose	10.94	0.00	0.584	171.3	175.6	$^1C_4$	1.000
	17.66	6.73	0.757	102.2	90.0	$^5S_1/^{2,5}B$	0.000
	18.21	7.27	0.502	115.5	14.9	$^4C_1$	0.000
	18.36	7.42	0.683	342.6	96.1	$^OS_2/^{3,O}B$	0.000
Average α:	11.19	0.25					0.396
Average β:	10.94	0.00					0.604
α-Tyvelose	11.92	0.00	0.550	269.9	8.7	$^4C_1$	0.905
	13.35	1.43	0.550	261.7	173.9	$^1C_4$	0.081
	14.37	2.45	0.771	328.0	89.4	$^OS_2$	0.014
	17.08	5.16	0.772	212.2	90.4	$^1S_3$	0.000
β-Tyvelose	11.25	0.00	0.583	343.6	5.0	$^4C_1$	0.998
	15.10	3.86	0.512	336.9	171.8	$^1C_4$	0.001
	16.59	5.34	0.760	26.2	86.4	$^3S_1$	0.000
	17.17	5.92	0.749	277.6	88.1	$^1S_5/B_{2,5}$	0.000
Average α:	12.07	0.82					0.200
Average β:	11.26	0.00					0.800

rhamnose, respectively. In no case do these second forms exceed 0.2% of the total in any of the four sugars.

The calculated β anomeric fraction exceeds 0.8 in abequose, L-fucose, paratose, D-quinovose, and tyvelose, is somewhat over half in L-rhamnose, and is slightly under half in D-digitoxose (Table 1).

NMR hydrogen–hydrogen coupling constants averaged by Bolzmann distributions of the local minima are shown in Table 2 for both anomers of the seven sugars.

4. Discussion

Modeling of deoxy and dideoxy structures is a convenient way to determine the effects of the hydroxyl groups of a ring on its conformation. For example, fucose, quinovose, and rhamnose are identical to galactose, glucose, and mannose, respectively, except for their missing 6-OH groups. Computation reveals that the lowest energy conformer of D-quinovose is $^4C_1$, while $^1C_4$ is the dominant conformer for L-fucose and L-rhamnose (Table 1), a result that is expected since the ring conformation of L-enantiomers is inverted compared to their equivalent D-forms. Both crystallographic (Fig. 3) and NMR studies (Table 2) confirm the dominance of the $^1C_4$ conformation for L-fucose[18–23,40,41] and L-rhamnose,[24–35,40–42] and NMR spectroscopy confirms that the $^4C_1$ form is dominant for D-quinovose.[40,41] Since the 6-methyl group is relatively bulky even after replacing its hydroxyl group with a hydrogen atom, and since it is external to the ring, one would not expect the lowest energy conformations of these deoxyhexoses to differ greatly from their oxygenated counterparts, and indeed this is the case, the $^4C_1$ conformations determined experimentally[1,4,66–68] and calculated using MM3[53] also being overwhelmingly dominant in aqueous solutions of D-galactose, D-glucose, and D-mannose.

A more sensitive test of the effect of replacing the 6-OH group with a hydrogen atom is to compare the relative energies between the dominant and remaining chair conformers of the two anomers of L-fucose, D-quinovose, and L-rhamnose with those of their parent oxygenated hexoses. In all six cases the relative energies of the secondary chair forms of the deoxyhexoses (Table 1) decrease by well less than 1 kcal/mol from the equivalent relative energies of the secondary chair forms of the parent hexoses.[53]

Further substitution of the 3-OH group with a hydrogen atom to produce the D-dideoxyhexoses abequose, paratose, and tyvelose leads to an enrichment of the $^1C_4$

Table 2
Hydrogen–hydrogen coupling constants ($J_{i,j}$, Hz) of deoxy- and dideoxypyranoses calculated from the MM3(92) conformer distributions and compared with experimental values

6-Deoxy sugars	J_{12}	J_{23}	J_{34}	J_{45}	Reference
α-L-Fucose	3.6	9.1	2.9	0.6	this work
	3.0				40 [a]
	2.8				41 [b]
β-L-Fucose	7.1	9.0	3.0	0.6	this work
	7.5				40 [a]
	8.2	10.0	3.6	0.8	41 [b]
α-D-Quinovose	3.5	9.0	8.8	8.9	this work
	3.5				40 [a]
	3.6	9.2	9.5	9.6	41 [b]
β-D-Quinovose	7.2	8.9	8.6	8.9	this work
	7.8				40 [a]
	8.2	9.8	9.5	9.5	41 [b]
α-L-Rhamnose	2.3	3.2	8.9	9.0	this work
	1.7				40 [a]
	1.8	3.5	9.6	9.6	42 [c]
	1.7	3.5	9.6	9.6	42 [d]
	1.9	3.5	9.4	9.5	42 [e]
	1.6	3.5	9.5	9.5	41 [b]
	1.7	3.7	9.9	9.9	30 [f]
β-L-Rhamnose	1.3	3.0	8.6	8.9	this work
	1.1				40 [a]
	1.1	3.5	9.5	9.6	42 [c]
	1.1	3.5	9.5	9.5	42 [e]
	0.9	3.3	9.2		41 [b]
	1.1	3.3	9.3		30 [f]

2,6-Dideoxy sugar	J_{12u}	J_{12d}	J_{2u3}	J_{2d3}	J_{34}	J_{45}	
α-D-Digitoxose	3.8	2.4	2.5	3.9	2.7	8.8	this work
	3.4	1.2	3.4	3.2	3.5	9.8	43 [g]
	3.7	2.0	3.2	3.6	3.0	9.0	45 [h]
β-D-Digitoxose	10.3	3.5	2.6	3.7	2.9	8.7	This work
	9.2	2.5	2.7	3.4	3.0	9.4	44 [i]
	9.6	2.1	2.7	3.5	3.1	9.4	45 [h]

3,6-Dideoxy sugars	J_{12}	J_{23u}	J_{23d}	J_{3u4}	J_{3d4}	J_{45}	
α-Abequose	3.3	5.0	10.8	3.6	2.7	0.8	this work
β-Abequose	6.7	5.2	10.9	3.2	2.8	0.7	this work
α-Paratose	2.8	4.4	9.2	4.4	9.1	6.7	this work
β-Paratose	6.7	5.2	10.9	5.0	11.0	8.4	this work
	8.7	3.7	10.5	3.7	10.5		48 [j]
α-Tyvelose	2.5	3.8	3.1	4.6	10.3	7.9	this work
	1.7	3.4	3.2	4.5	11.1	9.4	39 [k]
		3.5	3.0	3.5	10.9		47 [l]
β-Tyvelose	1.3	3.4	2.6	5.2	10.9	8.5	this work
	1.2	4.0	3.0	4.0	10.9	8.8	47 [l]

[a] L-Fucose, D-quinovose, or L-rhamnose. ^{1}H NMR, 100 MHz, D_2O.
[b] Methyl α- or β-D-fucopyranoside, methyl α- or β-D-quinovopyranoside, or methyl α- or β-D-rhamnopyranoside, ^{1}H NMR, 400 MHz, D_2O.
[c] L-Rhamnose. ^{1}H NMR, 300 MHz, D_2O.
[d] Methyl α-L-rhamnopyranoside. ^{1}H NMR, 300 MHz, D_2O.
[e] α- or β-L-rhamnopyranosyl-(1→4)-D-galactose. ^{1}H NMR, 300 MHz, D_2O.
[f] 1,2,4-Tri-*O*-acetyl-α-L-rhamnopyranose or 1,2,3-tri-*O*-acetyl-β-L-rhamnopyranose. ^{13}C NMR, 270 MHz, $CDCl_3$.
[g] Methyl α-D-digitoxopyranoside. ^{1}H NMR, 100 MHz, $CDCl_3$.
[h] α- and β-D-digitoxopyranose. ^{1}H NMR, 400 MHz, Me_2SO-d_6.
[i] β-D-Digitoxose. ^{1}H NMR, 90 MHz, Me_2SO-d_6.
[j] Methyl β-paratopyranoside. ^{1}H NMR, 80 MHz, D_2O.
[k] Methyl α-tyvelopyranoside. ^{1}H NMR, 500 MHz, D_2O.
[l] Methyl α- or β-tyvelopyranoside. ^{1}H NMR, 360 MHz, $CDCl_3$.

form in all three α anomers, especially in α-paratose, although the $^4C_1$ conformers remain dominant (Table 1), as is experimentally found for paratose and tyvelose.[39,47,48] In all six anomeric forms, the relative energies of their $^1C_4$ conformers decrease from those of the parent deoxyhexoses by much more than is caused by the substitution of the 6-OH group, the decreases ranging from 2.3 kcal/mol in α-tyvelose to 5.4 kcal/mol in β-paratose (Table 1).

Two effects are responsible for these differences. The loss of the C-3 hydroxyl group forces a disruption of a hydrogen-bonding crown that exists around many pyranosyl rings in $^4C_1$ conformations. In addition, the $^1C_4$ conformation of paratose is stabilized by a strong 1,3-diaxial hydrogen bond between the C-2 and C-4 hydroxyl groups. This interaction is not possible for abequose or tyvelose, as either the C-2 or C-4 hydroxyl groups have opposite configurations. Although the dielectric constant has been elevated to reduce the influence of intramolecular hydrogen bonding and improve the comparison with condensed-phase systems, the effect is reduced to approximately half at $\varepsilon = 3.0$ and contributes to the observed differences.

Replacing the 2-OH and 6-OH groups of D-allose or D-altrose[53] with hydrogen atoms to yield D-digitoxose causes the relative energies between the dominant $^4C_1$ and secondary $^1C_4$ conformer to increase in α-D-digitoxose but to decrease in β-D-digitoxose (Table 1). This increases the proportion of the $^4C_1$ conformer of α-D-digitoxose compared to α-D-allose and α-D-altrose, but decreases the proportion of the $^4C_1$ conformer of β-D-digitoxose compared to β-D-allose and β-D-altrose. With both anomers, the $^4C_1$ conformer of D-digitoxose is approximately 97% of the total, and this is the dominant conformer found by diffraction[36–38] and by NMR spectroscopy.[43–46]

Because a partial crown of hydrogen bonding is still possible between the C-3 and C-4 hydroxyl groups, the loss of the C-2 hydroxyl group does not appear to have as large of an influence on the distribution of ring forms as the loss of the hydroxyl group at C-3.

A pure test of the effect of replacing the 2-OH group with a hydrogen atom, unencumbered by the parallel substitution of the 6-OH group, is to compare the relative energies between the $^4C_1$ and $^1C_4$ conformers of the two anomers of D-ribopyranose and 2-deoxy-D-ribopyranose,[57] which have equatorial 3-OH groups as in D-digitoxose. The relative energy of the $^1C_4$ conformer of 2-deoxy-α-D-ribopyranose is more positive (less negative) than that of α-D-ribopyranose, while the opposite is true for the corresponding β anomers. This is also found when the relative energies of the $^1C_4$ conformers of the two anomers of D-digitoxose are compared with those of D-allose and D-altrose.[53] This suggests that the larger change in relative energies is caused by the substitution of the 2-OH group rather than the substitution of a 6-OH group by a hydrogen atom, since essentially the same changes in relative energies are found when 6-OH groups are present, as in D-ribopyranose and 2-deoxy-D-ribopyranose, as when they are absent, as in D-allose, D-altrose, and D-digitoxose.

Overall, modeled proton–proton coupling constants agreed well with experimental values. Except for β-paratose, the root-mean-squared differences between modeled values, based on the MM3-calculated steric energy predicted conformer distribution and the Haasnoot et al. coupling constant model,[65] and experimental values was between 0.4 and 0.8 Hz. The Karplus model[65] has an expected deviation of 0.35–0.5 Hz, and the differences observed (0.4–0.8 Hz) are similar to those for other MM3-modeled carbohydrate rings.[53–59] For β-paratose, the difference was 1.3 Hz. The largest single contributor to this difference was 2.0 Hz for the coupling between the protons at C-1 and C-2. Because the MM3-calculated conformer distribution was dominated by the $^4C_1$ form, the J_{12} coupling constant for the conformer population was essentially the same as for that chair form (6.7 Hz). The discrepancy with experiment did not appear to be due to a skewed conformer distribution, as none of the other local low-energy structures had a J_{12} value that would have improved the comparison. Because the experimental work was conducted on the methyl β-paratopyranoside and the modeling was on the unsubstituted sugar, the difference is most likely

associated with the substitution at C-1. Unfortunately, no NMR data for β-abequopyranose or its methyl glycoside, which has the same relative configuration about this part of the molecule, was available for comparison.

The MM3-computed values for the anomeric ratios of the pyranosyl forms of all three deoxyhexoses can be compared with experimental data. MM3 gives 81% β-L-fucose (Table 1), while Angyal and Pickles[40] by ^{1}H NMR spectroscopy found 67% β-L-fucose in D_2O, along with a small percentage in the furanosyl form. Disregarding the latter, the β anomer is 70% of the aqueous solution. HPLC with a graphitized carbon column of an aqueous solution of L-fucose gave 72% β anomer.[69] D-Quinovose is 86% β anomer by MM3 and 64% by ^{1}H NMR.[40] With L-rhamnose, MM3 gives 60% β anomer, ^{1}H NMR in D_2O finds 40%,[40] and the graphitized carbon column gives 27%.[69] These comparisons further demonstrate the propensity of MM3(92) to overestimate the β anomeric concentration of aldohexoses in the $^4C_1$ form by 10% or more.[53]

This effect appears to be associated with MM3 functionality for calculating anomeric sequences, as the overpredicted form always has a trans orientation of the C-5–O-5–C-1–O-1 torsion, and the underpredicted form always has a gauche orientation for this torsion.[58]

When L-fucose and L-rhamnose were eluted from a cation-exchange column by a 20:80 (v/v) solution of water and acetonitrile,[70] equilibrium concentrations of 32% β-L-fucose and 82% β-L-rhamnose were measured. Clearly the solvent greatly affects the anomeric equilibrium.

^{1}H and ^{13}C NMR spectroscopy revealed that an equilibrium solution of D-digitoxose in Me_2SO-d_6 consists of an average of 12% α-pyranose, 66% β-pyranose, 9% α-furanose, and 13% β-furanose,[45,46] compared to the MM3-computed value of 52% α-pyranose and 48% β-pyranose, furanosyl forms not being considered (Table 1). The differences can again be rationalized by solvent effects and the tendency of MM3 to overpredict the β anomer for sugars existing predominantly in the $^4C_1$ form. It is worth noting that the removal of the 2-OH group, as with digitoxose, tends to increase the composition of furanosyl forms in solution, Angyal and Pickles[40] having found that 3-deoxy-D-*ribo*-hexofuranose (3-deoxy-D-glucofuranose) exists at nearly 30% in aqueous solution, while the furanosyl form is scarcely present in aqueous solutions of D-glucose.

References

1. Rudrum, M.; Shaw, D. F. *J. Chem. Soc.* **1965**, 52–57.
2. Lemieux, R. U.; Stevens, J. D. *Can. J. Chem.* **1966**, *44*, 249–262.
3. Angyal, S. J.; Pickles, V. A. *Aust. J. Chem.* **1972**, *25*, 1695–1710.
4. Chu, S. S. U.; Jeffrey, G. A. *Acta Crystallogr., Sect. B* **1968**, *24*, 830–833.
5. Joshi, N. V.; Raghavendra Rao, V. S. *Biopolymers* **1979**, *18*, 2993–3004.
6. Tvaroška, I.; Kožár, T. *Theor. Chim. Acta* **1986**, *70*, 99–114.
7. Brady, J. W. *J. Am. Chem. Soc.* **1989**, *111*, 5155–5165.
8. Cramer, C. J.; Truhlar, D. G. *J. Am. Chem. Soc.* **1993**, *115*, 5745–5753.
9. Roszkowski, W.; Beuth, J.; Ko, H. L.; Uhlenbruck, G.; Pulverer, G. *Experientia* **1989**, *45*, 584–588.
10. Kamel, M.; Serafi, T. *Clin. Exp. Rheumatol.* **1995**, *13*, 243–246.
11. Fang, Y.; Chai, W.; Chen, S.; He, Y.; Zhao, L.; Peng, J.; Huang, H.; Xin, B. *Carbohydr. Res.* **1993**, *245*, 259–270.
12. Pathirana, C.; Jensen, P. R.; Dwight, R.; Fenical, W. *J. Org. Chem.* **1992**, *57*, 740–742.
13. Voet, D.; Voet, J. G. *Biochemistry*, 2nd ed.; Wiley: New York, 1995; p. 527.
14. Thorson, J. S.; Lo, S. F.; Ploux, O.; He, X.; Liu, H. W. *J. Bacteriol.* **1994**, *176*, 5483–5493.
15. Liu, H.; Thorson, J. S. *Annu. Rev. Microbiol.* **1994**, *48*, 223–256.
16. Hallis, T.; Liu, H. *J. Am. Chem. Soc.* **1999**, *121*, 6765–6766.
17. Fullerton, D. S.; Kihara, M.; Deffo, T.; Kitatsuji, E.; Ahmed, K.; Simat, B.; From, A. H. L.; Rohrer, D. C. *J. Med. Chem.* **1984**, *27*, 256–261.
18. Cook, W. J.; Bugg, C. E. *Biochim. Biophys. Acta* **1975**, *389*, 428–435.
19. Longchambon, F.; Ohannessian, J.; Avenel, D.; Neuman, A. *Acta Crystallogr., Sect. B* **1975**, *31*, 2623–2627.
20. Longchambon, F.; Gillier-Pandraud, H.; Becker, P. *Acta Crystallogr., Sect. B* **1977**, *33*, 2094–2096.
21. Lamba, D.; Segre, R. L.; Fabrizi, G.; Matsuhiro, B. *Carbohydr. Res.* **1993**, *243*, 217–224.
22. Watt, D. K.; Brasch, D. J.; Larsen, D. S.; Melton, L. D.; Simpson, J. *Carbohydr. Res.* **1996**, *285*, 1–15.
23. Eriksson, L.; Stenutz, R.; Widmalm, G. *Acta Crystallogr., Sect. C* **2000**, *56*, 702–704.
24. Killean, R. C. G.; Lawrence, J. L.; Sharma, V. C. *Acta Crystallogr., Sect. B* **1971**, *27*, 1707–1710.
25. Takagi, S.; Jeffrey, G. A. *Acta Crystallogr., Sect. B* **1978**, *34*, 2551–2555.
26. Messerschmidt, A. *Crystallogr. Struct. Commun.* **1980**, *9*, 1185–1194.

27. Messerschmidt, A.; Megges, R.; Schrauber, H. *Crystallogr. Struct. Comm.* **1981**, *10*, 1041–1051.
28. Krajewski, J. W.; Urbańczyk-Lipkowska, Z.; Gluziński, P.; Zamijski, A.; Stadnicka, K. *Carbohydr. Res.* **1983**, *117*, 13–22.
29. Wiedenfeld, H.; Knoch, F.; Naidis, I.; Kopp, B. *Sci. Pharm.* **1987**, *55*, 167–176.
30. Lee, E.; Galvin, N.; McArdle, P.; Cunningham, D. *Carbohydr. Res.* **1990**, *197*, 270–275.
31. Yamada, H.; Nishizawa, M.; Katayama, C. *Tetrahedron Lett.* **1992**, *33*, 4009–4010.
32. Shalaby, M. A.; Fronczek, F. R.; Younathan, E. S. *Carbohydr. Res.* **1993**, *258*, 267–274.
33. Shalaby, M. A.; Fronczek, F. R.; Younathan, E. S. *Carbohydr. Res.* **1994**, *264*, 173–180.
34. Ashton, P. R.; Brown, C. L.; Menzer, S.; Nepogodiev, S. A.; Stoddart, J. F.; Williams, D. J. *Chem. Eur. J.* **1996**, *2*, 580–591.
35. Ashton, P. R.; Cantrill, S. J.; Gattuso, G.; Menzer, S.; Nepogodiev, S. A.; Shipway, A. N.; Stoddart, J. F.; Williams, D. J. *Chem. Eur. J.* **1997**, *3*, 1299–1314.
36. Kanters, J. A.; Batenburg, L. M. J.; Gaykema, W. P. J.; Roelofsen, G. *Acta Crystallogr., Sect. B* **1978**, *34*, 3049–3053.
37. Go, K.; Kartha, G. *Crystallogr. Struct. Commun.* **1982**, *11*, 279–284.
38. Go, K.; Bhandary, K. K. *Acta Crystallogr., Sect. B* **1989**, *45*, 306–312.
39. Birnbaum, G. R.; Bundle, D. R. *Can. J. Chem.* **1985**, *63*, 739–744.
40. Angyal, S. J.; Pickles, V. A. *Aust. J. Chem.* **1972**, *25*, 1711–1718.
41. Bock, K.; Thøgersen, H. *Annu. Rep. NMR Spectrosc.* **1982**, *13*, 1–57.
42. De Bruyn, A.; Anteunis, M.; De Gussem, R.; Dutton, G. G. S. *Carbohydr. Res.* **1976**, *47*, 158–163.
43. Cheung, T. M.; Horton, D.; Weckerle, W. *Carbohydr. Res.* **1977**, *58*, 139–151.
44. Ferrige, A. G.; Lindon, J. C. *Spectrosc. Lett.* **1980**, *13*, 339–345.
45. Coxon, B. *J. Carbohydr. Chem.* **1984**, *3*, 525–543.
46. Coxon, B. *Magn. Reson. Chem.* **1986**, *24*, 1008–1012.
47. Probert, M. A.; Zhang, J.; Bundle, D. R. *Carbohydr. Res.* **1996**, *296*, 149–170.
48. Bundle, D. R. *J. Chem. Soc., Perkin Trans. 1* **1979**, 2751–2755.
49. Csonka, G.; Éliás, K.; Csizmadia, I. *J. Comput. Chem.* **1996**, *18*, 330–342.
50. Allinger, N. L.; Yuh, Y. H.; Lii, J.-H. *J. Am. Chem. Soc.* **1989**, *111*, 8551–8566.
51. Lii, J.-H.; Allinger, N. L. *J. Am. Chem. Soc.* **1989**, *111*, 8566–8575.
52. Allinger, N. L.; Rahman, M.; Lii, J.-H. *J. Am. Chem. Soc.* **1990**, *112*, 8293–8307.
53. Dowd, M. K.; French, A. D.; Reilly, P. J. *Carbohydr. Res.* **1994**, *264*, 1–19.
54. Dowd, M. K.; French, A. D.; Reilly, P. J. *Aust. J. Chem.* **1996**, *49*, 327–335.
55. French, A. D.; Dowd, M. K. *J. Comput. Chem.* **1994**, *15*, 561–570.
56. French, A. D.; Dowd, M. K.; Reilly, P. J. *J. Mol. Struct. (Theochem)* **1997**, *395–396*, 271–287.
57. Dowd, M. K.; French, A. D.; Reilly, P. J. *J. Carbohydr. Chem.* **2000**, *19*, 1091–1114.
58. Dowd, M. K.; Rockey, W. M.; French, A. D.; Reilly, P. J. *J. Carbohydr. Chem.* (in press).
59. Cros, S.; Hervé de Penhoat, C.; Pérez, S.; Imberty, A. *Carbohydr. Res.* **1993**, *248*, 81–93.
60. French, A. D.; Dowd, M. K. *J. Mol. Struct. (Theochem)* **1993**, *186*, 183–201.
61. Kremer, D.; Pople, J. A. *J. Am. Chem. Soc.* **1975**, *97*, 1354–1358.
62. Jeffrey, G. A.; Yates, J. H. *Carbohydr. Res.* **1979**, *74*, 319–322.
63. Pickett, H. M.; Strauss, H. L. *J. Am. Chem. Soc.* **1970**, *92*, 7281–7290.
64. Strauss, H. L. *J. Chem. Educ.* **1971**, *48*, 221–223.
65. Haasnoot, C. A. G.; de Leeuw, F. A. A. M.; Altona, C. *Tetrahedron* **1980**, *36*, 2783–2792.
66. Longchambon, F.; Avenel, D.; Neuman, A. *Acta Crystallogr., Sect. B* **1976**, *32*, 1822–1826.
67. Sheldrick, B. *Acta Crystallogr., Sect. B* **1976**, *32*, 1016–1020.
68. Brown, G. M.; Levy, H. A. *Acta Crystallogr., Sect. B* **1979**, *35*, 656–659.
69. Koizumi, K.; Okada, Y.; Fukuda, M. *Carbohydr. Res.* **1991**, *215*, 67–80.
70. Honda, S.; Suzuki, S.; Kakehi, K. *J. Chromatogr.* **1984**, *291*, 317–325.